3d electron microscopy in injured rat brain validates white matter microstructure metrics from diffusion MRI

Ricardo Coronado-Leija[1], Ali Abdollahzadeh[1], Hong-Hsi Lee[2], Santiago Coelho[1], Benjamin Ades-Aron[1], Ying Liao[1], Raimo A Salo[3], Jussi Tohka[3], Alejandra Sierra[3], Dmitry S Novikov[1], and Els Fieremans[1]

[1]Bernard and Irene Schwartz Center for Biomedical Imaging, Department of Radiology, New York University School of Medicine, New York, NY, United States.

[2]Athinoula A. Martinos Center for Biomedical Imaging, Department of Radiology, Massachusetts General Hospital, Harvard Medical School, Boston, MA, United States.

[3]A. I. Virtanen Institute for Molecular Sciences, University of Eastern Finland, Kuopio, Finland.

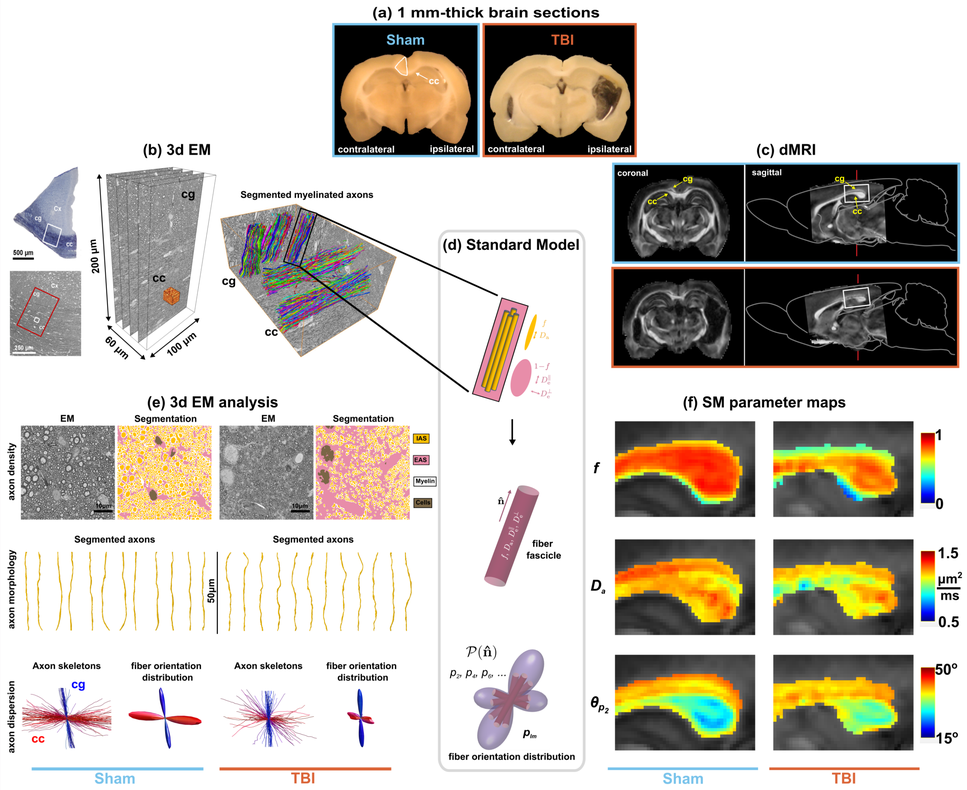

Fig. 1. *SM parameter maps reveal specific microstructure properties that correspond to 3d EM.*

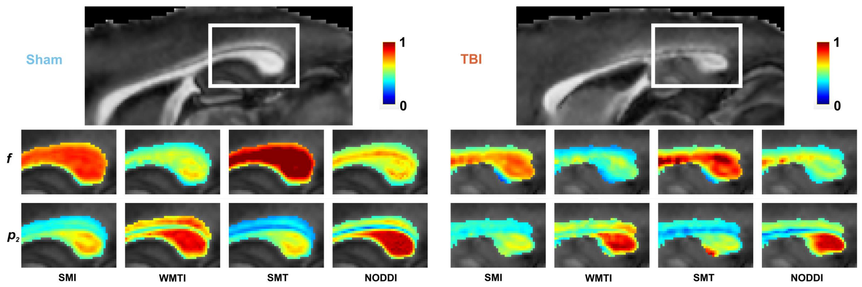

Fig. 2. *SM parameter maps obtained using different estimators: WMTI, NODDI, SMT & SMI*

Introduction

- Biophysical modeling of diffusion MRI[1-3] (dMRI) offers the exciting potential of bridging the gap between the macroscopic MRI resolution and microscopic cellular features, effectively turning the MRI scanner into a noninvasive *in vivo* microscope.
- In brain white matter (WM), the Standard Model (SM) interprets the dMRI signal in terms of axon dispersion, intra- and extra-axonal water fractions and diffusivities, see **Fig. 1d**. SM is described by parameters $\boldsymbol{f}$, $\boldsymbol{D_a}$, $\boldsymbol{D_e^{\parallel}}$, $\boldsymbol{D_e^{\perp}}$, and the FOD $\boldsymbol{\mathcal{P}(n)}$.
- In this work, we perform a comprehensive histological validation of the sensitivity and specificity of the SM parameters, by characterizing WM microstructure in sham and injured rat brains using *ex vivo* dMRI and 3d electron microscopy (EM).

Methods

- **Animal preparation**[4,5]. Traumatic Brain Injury (TBI) was induced by a lateral fluid-percussion injury in three adult rats, while two rats went through a sham-operation that included all surgical procedures except the impact, **Fig. 1a**.
- **dMRI imaging**: *Ex vivo* dMRI data (150x150x150 μm^3) was acquired on a 9.4T magnet at room temperature, 21ºC, using 42 diffusion gradient directions for b= 2, 3, and 4 ms/μm^2; with 3 non-diffusion weighted images. δ/Δ=6/11.5 ms, TR/TE=1000/35 ms. FA maps for sham and TBI rats are shown in **Fig. 1c**.
- **dMRI processing:** Images were denoised[6], corrected for Gibbs-ringing[7], B1 inhomogeneities[8] and motion distortions[9]. SM parameters were obtained using four different estimators that handle the known degeneracies of the problem[10]: WMTI[11], NODDI[12], SMT[13] and SMI[14-16]. SM maps differences are shown in **Fig. 2.**
- **3d EM imaging and segmentation**: Ten WM samples, two from each rat, were prepared for serial block-face-scanning electron microscopy imaging[4,5], as shown in **Fig. 1b.** Large tissue volumes of 200x100x65 μm^3 were imaged with resolution of 50x50x50 nm^3. Myelin and myelinated axons were automatically segmented using the deep-learning pipeline DeepACSON[17,18].
- **Microstructural metrics derived from 3d EM.** From 3d EM segmentations, the intra-axon volume fraction $\boldsymbol{f}$ was computed. From the segmented 3d axons[19], the diameter, the axial tortuosity $\boldsymbol{\Lambda_{\parallel}}$ from the cross-sectional area variations derived in ref20, dispersion angle $\boldsymbol{\theta}$, and fiber orientation distribution with their rotational invariants $\boldsymbol{p_l}$ were computed. Undulation based dispersion angle $\boldsymbol{\theta_u}$ was computed by first aligning all axons to the z-axis. $\boldsymbol{p_2}$ is approximately related to the dispersion angle[15,19] by $\boldsymbol{\cos^2\theta \approx \cos^2\theta_{p_2} = \frac{2p_2+1}{3}}$.

Results

- **Fig. 1e** shows reduction of axonal density, changes in axon morphology (diameter reduction, increased beading & undulation), and increase in dispersion for the TBI sample.
- Remarkably, these microstructural changes are also detected non-invasively by ex vivo MRI, as shown on the SM maps in **Fig. 1f** for $\boldsymbol{f}$, $\boldsymbol{D_a}$, and $\boldsymbol{\theta_{p_2}}$, and **Fig. 2.**
- Correspondence between 3d EM and dMRI metrics are observed in **Fig. 3** and **Fig. 4**:
  1. **Intra-axonal water fraction $\boldsymbol{f}$**[21,22]: SMI, WMTI and SMT show significant correlations with 3d EM $\boldsymbol{f}$ and don't correlated with $\boldsymbol{\widetilde{D}_a}$, and $\boldsymbol{\theta}$ metrics, showing specificity.
  2. **Dispersion angle $\boldsymbol{\theta_{p_2}}$**[5,25]: All methods show significant correlations 3d EM $\boldsymbol{\theta}$, but only SMI, SMT and NODDI show specificity, as WMTI $\boldsymbol{\theta_{p_2}}$ also correlates with histological $\boldsymbol{f}$.
  3. **Intra-axonal diffusivity $\boldsymbol{D_a}$**: SMI, WMTI and SMT show correlations with predicted $\boldsymbol{\widetilde{D}_a}$ from the axial tortuosity and undulation of the axons, assuming free diffusivity for perfect cylinders, in agreement with MC studies[20,23,24]. Only SMI $\boldsymbol{D_a}$ shows specificity.
  4. **Radial extra-axonal diffusivity $\boldsymbol{D_e^{\perp}}$**: the positive correlation between 3d EM $\boldsymbol{f}$ with SMI $\mathbf{D_e^{\perp}}$ contradicts the tortuosity relation[26,27] used by NODDI and SMT. Using functional relations between $\boldsymbol{D_e^{\perp}}$ and $\boldsymbol{f}$ is unjustified, and they rather should be estimated independently, particularly in pathological conditions.

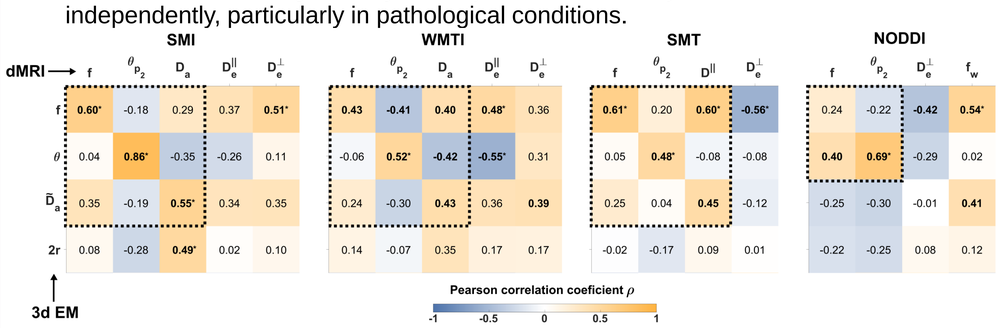

Fig. 3. *Pearson correlations between 3d EM histology derived metrics (rows) and dMRI estimated SM parameters (columns) for the different estimators. Significant correlation* (p<0.05) *are highlighted in* ***bold****, while * indicates that significance remains after adjusting for multiple comparisons using the false discovery rate.*

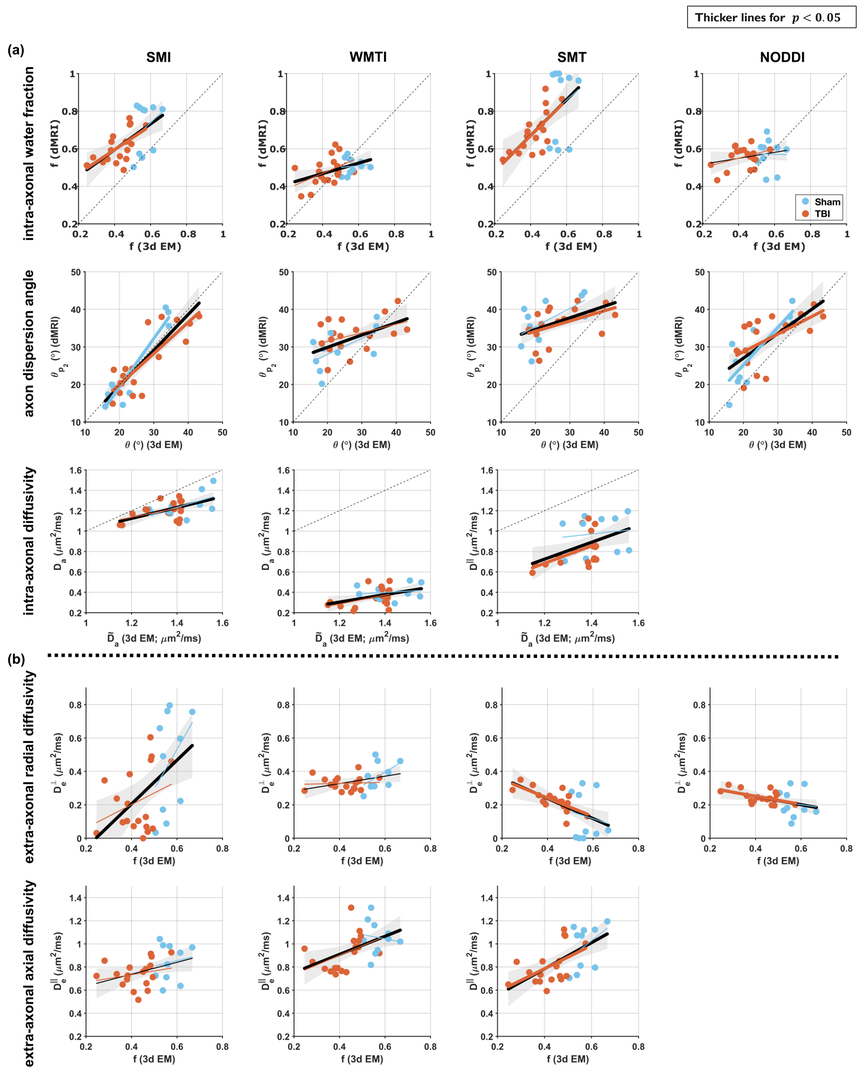

Fig. 4. *Scatter plots for dMRI derived parameters against histology metrics. (a) SM parameters $\boldsymbol{f}$, $\boldsymbol{D_a}$, and $\boldsymbol{\theta_{p_2}}$ from SMI, WMTI, SMT, and NODDI compared against their corresponding 3d EM metrics. (b) SM extra-axonal diffusivities $\boldsymbol{D_e^{\parallel}}$, $\boldsymbol{D_e^{\perp}}$ compared against histological $\boldsymbol{f}$.*

Conclusions

- We used 3d EM derived metrics on sham and injured rat brains to validate SM parameters from four publicly available estimators: WMTI, NODDI, SMT and SMI.
- All SM estimators provide SM parameters that correlate significantly (p<0.05) with their histological counterparts (except for NODDIs $\boldsymbol{f}$), indicating sensitivity.
- SMI shows the highest specificity by presenting smallest cross-correlations with other, non-corresponding histological features.

References

1 Novikov DS et al. NMR Biomed. 32 4 (2019); **2** Alexander DC et al. NMR Biomed. 32 4 (2019); **3** Jelescu IO and Budde MD. Front. Physics 5 (2017); **4** Salo RA et al. Neuroimage 172 (2018); **5** Salo RA et al. Neuroimage 225 (2021); **6** Veraart J et al. Neuroimage 142 (2016); **7** Kellner E et al. Magn. Reson. Med. 76 5 (2016); **8** Tustison NJ et al. IEEE Trans. Med. Imaging 29 6 (2010); **9** Avants BB et al. Med. Image Anal. 12 1 (2008); **10** Jelescu IO et al. Neuroimage 132 (2016); **11** Fieremans E et al. Neuroimage 58 1 (2011); **12** Zhang H et al. Neuroimage 61 4 (2012); **13** Kaden et al. Neuroimage 139 (2016); **14** Reisert M et al. Neuroimage 147 (2017); **15** Novikov DS Neuroimage 174 (2018); **16** Coelho et al. Neuroimage 257 (2022); **17** Abdollahzadeh A et al. Sci Rep 9 1 (2019); **18** Abdollahzadeh A et al. Commun Biol. 4 1 (2021); **19** Lee HH et al. Brain Struct Funct 224 4 (2019); **20** Abdollahzadeh A et al. ISMRM (2023); **21** Jelescu IO et al. Neuroimage 132 (2016); **22** Coronado-Leija R et al. ISMRM (2021); **23** Budde MD et al. Proc Natl Acad Sci. 107 32 (2010); **24** Lee HH. Commun Biol. 3 1 (2020); **25** Schilling KG et al. Neuroimage 165 (2018); **26** Sen et al. Geophysics 46 5 (1981); **27** Szafer A et al. Magn. Reson. Med. 33 5 (1995);

Research was supported by the National Institute of Neurological Disorders and Stroke of the NIH under awards R01 NS088040 and R21 NS081230, and by the Hirschl foundation, and was performed at the Center of Advanced Imaging Innovation and Research (CAI2R, www.cai2r.net), a Biomedical Technology Resource Center supported by NIBIB with the award P41 EB017183. A.S. was funded by the Academy of Finland (grant \#323385) and the Erkko Foundation. H.H.L. was funded by the Office of the Director of the NIH under award DP5 OD031854.

Center for Biomedical Imaging

CAI²R Center for Advanced Imaging Innovation and Research

NYU Grossman School of Medicine

Contact me at:
rleija@cimat.mx
Ricardo.CoronadoLeija@nyulangone.org